Journal of Molecular Structure 981 (2010) 130–138

Contents lists available at ScienceDirect

Journal of Molecular Structure

journal homepage: www.elsevier.com/locate/molstruc

Preparation, structure and microbial evaluation of metal complexes of the second generation quinolone antibacterial drug lomefloxacin

Sadeek A. Sadeek *, Walaa H. El-Shwiniy

Department of Chemistry, Faculty of Science, Zagazig University, Zagazig, Egypt

ARTICLE INFO

Article history:
Received 31 May 2010
Received in revised form 21 July 2010
Accepted 26 July 2010
Available online 4 August 2010

Keywords:
LFX
TGA
UV–Vis. spectra
Infrared
Kinetic parameters
^{1}H NMR

ABSTRACT

Lomefloxacinate of Y(III), Zr(IV) and U(VI) were isolated as solids with the general formula; $[Y(LFX)_2Cl_2]Cl{\cdot}12H_2O$, $[ZrO(LFX)_2Cl]Cl{\cdot}15H_2O$ and $[UO_2(LFX)_3](NO_3)_2{\cdot}4H_2O$. The new synthesized complexes were characterized with physicochemical and diverse spectroscopic techniques (IR, UV–Vis. and ^{1}H NMR spectroscopies) as well as thermal analyses. In these complexes lomefloxacin act as bidentate ligand bound to the metal ions through the pyridone oxygen and one carboxylate oxygen. The kinetic parameters of thermogravimetric (TGA) and its differential (DTG), such as entropy of activation, activation energy, enthalpy of activation and Gibbs free energy evaluated by using *Coats–Redfern* and *Horowitz–Metzger* equations for free lomefloxacin and three complexes were carried out. The bond stretching force constant and length of the U=O bond for the $[UO_2(LFX)_3](NO_3)_2{\cdot}4H_2O$ complex were calculated. The antimicrobial activity of lomefloxacin and its metal complexes was tested against different bacterial species, such as *Staphylococcus aureus* (*S. aureus*), *Escherichia coli* (*E. coli*) and *Pseudomonas aeruginosa* (*P. aeruginosa*) as Gram-positive and Gram-negative bacterial species and also against two species of antifungal, *penicillium* (*P. rotatum*) and *trichoderma* (*T. sp.*). The three complexes are of a good action against three bacterial species but the Y(III) complex exhibit excellent activity against *Pseudomonas aeruginosa* (*P. aeruginosa*), when compared to the free lomefloxacin.

1. Introduction

Fluoroquinolones belong to a group of synthetic antimicrobial agents being clinically used over the past thirty years and derived from basic structure of nalidixic acid and have substituents at N-1, C-5, C-7; position 8 and a fluorine atom at position 6. Some fluoroquinolones have been used in the development of anticancer drugs, and others have demonstrated anti-HIV activity [1–3].

Fluoroquinolones inhibit the bacterial DNA gyrase or the topoisomerase IV enzyme, resulting the inhibition of DNA replication and transcription [4–7]. Fluorine atom at position 6 enhances gyrase inhibition and cell penetration. Piperazinyl substituents provide activity against Gram-negative bacteria and pyrrolidinyl moity is active against Gram-positive cocci. The function substituted at position 8 is to control anaerobe activity [7].

The complexation of lomefloxacin with five metal ions (Al^{3+}, Ca^{2+}, Mg^{2+}, Bi^{3+}, and Fe^{3+}) commonly found in antacid or vitamin preparations has been studied. The pharmaceutical and biopharmaceutical implications of the effects of metal ion complexation on the aqueous solubility of lomefloxacin are discussed [8]. The binding reactions of lomefloxacin–copper(II) complex (LFX–Cu) or LFX to bovine serum albumin (BSA) in physiological solution were investigated by multi-spectroscopy. Copper ion plays an important role in organism's growth, cell division, protein synthesized, the activity of metal enzymes and induce the conformation of nucleic acid changed [9].

Lomefloxacin hydrochloride (Formula 1) sold under the following brand names in English speaking countries Maxaquin, Okacyn, Uniquin is one of the second generation drug of the quinolone antibiotics, transcriptase inhibitor and stable under ordinary conditions with color off – white to yellow crystals.

The crystal structures of several free quinolone molecules have been determined [10–14]. It is interesting to note that in most cases the carboxylic group is not deprotonated and the hydrogen atom of this group is hydrogen bonded to an adjacent 4-oxo atom. In a few examples [15–18], the carboxylic group is protonated and the molecule thus exists in a zwitterionic form with protonated terminal nitrogen of the piperazine ring in a solid state.

Crystal structures of quinolone complexes indicate that neutral quinolones in the zwitterionic state are capable of forming simple complexes [19–25]. The mechanism of the interaction between quinolone and metal cations was chelation between the metal and the 4-oxo and adjacent carbonyl groups. Since these functional groups are required for antibacterial activity. Also the crystal structure of free lomefloxacin was used together with ^{1}H NMR data on

* Corresponding author.
E-mail address: Sadeek59@yahoo.com (S.A. Sadeek).

0022-2860/$ - see front matter © 2010 Elsevier B.V. All rights reserved.
doi:10.1016/j.molstruc.2010.07.041

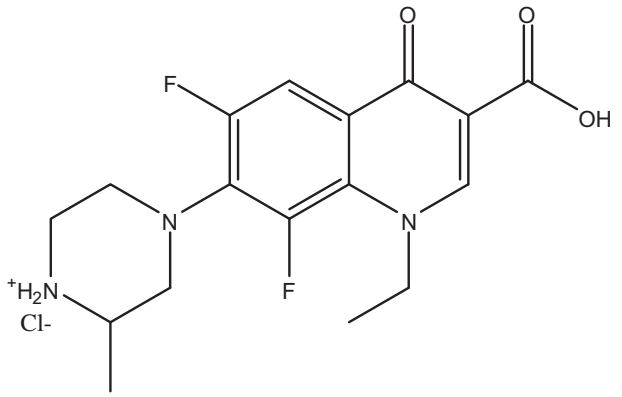

Formula 1. 4-(3-Carboxy-1-ethyl-6,8-difluoro-4-oxo-1,4-dihydroquinolin-7-yl)-2-methylpiperazin-1-iumchloride.

the aluminum complexes in molecular modeling of the lomefloxacin-Al (3:1) complex [14]. The authors suggested that three lomefloxacin molecules are coordinated to aluminum through carboxylic oxygen and 4-keto oxygen. The synthesis and characterization of new metal complexes with fluoroquinolones antibacterial agents are of great importance for understanding the drug-metal ion interaction and taking into account their potential pharmacological use.

To continue our investigation in this area [26–30], we report in the present article, the isolation and characterization of new metal complexes formed from the interaction of lomefloxacin with Y(III), Zr(IV) and U(VI) in the solvent. The prepared solid complexes are characterized using spectroscopic and thermal analysis techniques. The thermal behavior of these complexes was also studied. The antibacterial activity of the investigated complexes was tested against two Gram-negative bacteria such as *Escherichia coli* (*E. coli*) and *Pseudomonas aeruginosa* (*P. aeruginosa*) and one Gram-positive species *Staphylococcus aureus* (*S. aureus*) and antifungal activity was also investigated against two species, *penicillium* (*P. rotatum*) and *trichoderma* (*T. sp.*).

2. Materials and methods

Metal salts and solvents were purchased from Merck Germany. lomefloxacin was obtained from Sigma, these materials used without further purification.

The infrared spectra of the three solid complexes, lomefloxacin and the final products of the thermogravimetric analysis were recorded from KBr discs using FTIR 460 plus, ^{1}H NMR spectra were recorded on Varian Mercury VX-300 NMR Spectrometer using DMSO-d_6 as solvent. C, H, N and halogen elemental analysis were carried out on a Perkin Elmer CHN 2400. The percentage of Y(III), Zr(IV) and U(VI) metal ions were determined gravimetrically by transforming the solid products into oxide, and also determined by using atomic absorption method. A spectrometer model PYE-UNICAM SP 1900 fitted with the corresponding lamp was used for this purposed. Electronic spectra of lomefloxacin and the isolated solid complexes were obtained in the region of 800–200 nm using UV-3101PC Shimadzu. Thermogravimetric (TGA) and differential (DTG) thermogravimetric analyses were carried out under N_2-atmosphere using detectors model TGA-50H Shimadzu. The rate of heating of the sample was kept at 10 °C/min. Molar conductivities in DMSO at 7.0×10^{-4} M were measured on CONSORT K410.

2.1. Synthesis of lomefloxacin metal complexes

An ethanolic solution (20 ml) of lomefloxacin hydrochloride (1 mmol, 0.3878 g) and NaOH (1 mmol, 0.04 g) was added to an ethanolic solution of YCl_3 (0.5 mmol, 0.0977 g) and the reaction mixture was stirred for 3 days at 30 °C in water bath. The solution was left for slow evaporation, after that a yellowish white $[Y(LFX)_2Cl_2]Cl{\cdot}12H_2O$ product was deposited.The solid obtained was filtered under vacuum, washed with ethanol and dried. In a similar way, the Faint yellowish and Light green $[ZrO(LFX)_2Cl]Cl{\cdot}15H_2O$ and $[UO_2(LFX)_3](NO_3)_2{\cdot}4H_2O$ complexes were prepared by using methanol and acetone as a solvent instead of ethanol and using $ZrOCl_2{\cdot}8H_2O$ and $UO_2(NO_3)_2{\cdot}6H_2O$ in 1:2 and 1:3 M ratios. Unfortunately we were not able to obtained appropriate monocrystals to perform X-ray diffraction analysis. Qualitative black ring test for ionic nitrate using freshly prepared $FeSO_4$ solution and concentrated sulfuric acid, a black ring of $FeSO_4{\cdot}NO$ is formed led to the presence of nitrate as counter ions in the uranyl/LFX complex and for the other complexes the qualitative reactions revealed the presence of chloride as counter ions. The three complexes were characterized by their elemental analysis, infrared, electronic, ^{1}H NMR and thermal analyses.

2.2. Antimicrobial activity

Antibacterial activity of the ligand and its metal complexes was investigated by a previously reported modified method of Beecher and Wong [31], against different bacterial species, such as *S. aureus*, *E. coli* and *P. aeruginosa* and antifungal screening was studied against two species, *P. rotatum* and *T. sp*. The tested microorganisms isolates were isolated from Egyptian soil and identified according to the standard mycological and bacteriological keys for identification of fungi and bacteria as stock cultures in the microbiology laboratory, Faculty of Science, Zagazig University. The nutrient agar medium for antibacterial was (0.5% Peptone, 0.1% Beef extract, 0.2% Yeast extract, 0.5% NaCl and 1.5% Agar–Agar) and for antifungal (3% Sucrose, 0.3% $NaNO_3$, 0.1% K_2HPO_4, 0.05% KCl, 0.001% $FeSO_4$, 2% Agar–Agar) was prepared and then cooled to 47 °C and seeded with tested microorganisms. After solidification 5 mm diameter holes were punched by a sterile cork-borer. The investigated compounds, i.e., ligand and their com-

Table 1
Elemental analysis and physico-analytical data of lomefloxacin (LFX) and its metal complexes.

Compounds MWt. (MF.)	Yield%	Mp (°C)	Color	Content (calculated) found				
				%C	%H	%N	%M	%Cl
LFX	–	110	White	(52.60)	(5.16)	(10.83)	–	(9.14)
387.801 ($C_{17}H_{20}N_3O_3F_2Cl$)				52.59	5.16	10.82		9.14
$[Y(LFX)_2Cl_2]Cl{\cdot}2H_2O$	79.80	170	Yellowish white	(36.65)	(5.59)	(7.55)	(7.99)	(9.57)
1113.4 ($C_{34}H_{62}N_6O_{18}F_4Cl_3Y$)				36.63	5.59	7.51	7.99	9.54
$[ZrO(LFX)_2Cl]Cl{\cdot}15H_2O$	90.20	190	Faint yellowish	(35.47)	(5.91)	(7.30)	(7.93)	(6.17)
1150.22 ($C_{34}H_{68}N_6O_{22}F_4Cl_2Zr$)				35.47	5.89	7.30	7.91	6.15
$[UO_2(LFX)_3](NO_3)_2{\cdot}4H_2O$	69.20	180	Light green	(40.29)	(4.28)	(10.14)	(15.67)	–
1519 ($C_{51}H_{65}N_{11}O_{21}F_6U$)				40.27	4.28	10.12	15.66	

plexes, were introduced in Petri-dishes (only 0.1 ml) after dissolving in DMSO at 7.0×10^{-4} M. These culture plates were then incubated at 37 °C for 20 h for bacteria and for 7 days at 30 °C for fungi. The activity was determined by measuring the diameter of the inhibition zone (in mm). Growth inhibition was calculated with reference to the positive control, i.e., lomefloxacin.

3. Results and discussion

Lomefloxacinates of Y(III), Zr(IV) and U(VI) were prepared as solids of a color characteristic of the metal ions. The prepared complexes are hydrates with various degrees of hydration and with a metal to ligand ratio a mounting to 1:2 for Y(III), Zr(IV) and 1:3 for U(VI). The structures of the complexes suggested from the elemental analysis agree well with their proposed formula (Table 1). The found values of elemental analysis agree well with the calculated percentage of C, H, N and halogen data are in a well agreement with each other and prove the molecular formulas of the prepared complexes. The physical characteristic of these complexes are given in Table 1. The molar conductance values of the lomefloxacin and their Y(III), Zr(IV) and U(VI) complexes were found at 56.18, 281.27, 253.66 and 293.18 S cm^2 mol^{-1} at 25 °C, respectively.

3.1. Infrared absorption studies

The infrared spectra of lomefloxacin and their $[Y(LFX)_2Cl_2]Cl{\cdot}12H_2O$, $[ZrO(LFX)_2Cl]Cl{\cdot}15H_2O$ and $[UO_2(LFX)_3](NO_3)_2{\cdot}4H_2O$ complexes are usually similar, Fig. 1. The presence of the broad water bands in the 3414–3438 cm^{-1} zone confirms the presence of water molecules in all complexes Table 2, however, the absence of the very strong absorption band at 1725 cm^{-1}, arising from the carboxylic group (COOH) for under investigation complexes, states

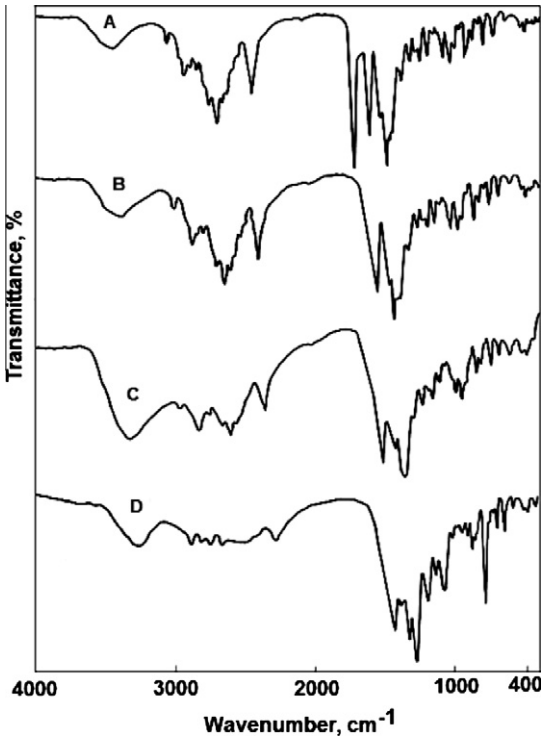

Fig. 1. Infrared spectra of: (A) lomefloxacin (LFX) as a ligand; (B) $[Y(LFX)_2Cl_2]Cl{\cdot}12H_2O$, (C) $[ZrO(LFX)_2Cl]Cl{\cdot}15H_2O$, and (D) $[UO_2(LFX)_3](NO_3)_2{\cdot}4H_2O$ complexes.

Table 2
Infrared frequencies[a] (cm^{-1}) and tentative assignments[b] for: (A) lomefloxacin (LFX) as a ligand; (B) $[Y(LFX)_2Cl_2]Cl{\cdot}12H_2O$, (C) $[ZrO(LFX)_2Cl]Cl{\cdot}5H_2O$, and (D) $[UO_2(LFX)_3](NO_3)_2{\cdot}H_2O$.

A	B	C	D	Assignments
3438m,br	3430m,br	3414m,br	3438m,br	ν(O–H); H_2O; COOH
3056m	3055m	3055m	3059m	ν(C–H); aromatic
2966vw	2928ms	2927m	2987w	ν(C–H); aliphatic
2933m	2891w	2849w	2926w	
2890w	2846m	2756w	2847m	
2845m	2759w	2700m		
2757m	2703ms			
2701ms				
2661w	2663w	2660vw	2461m	$\nu(-NH_2^+)$
2635vw	2588vw	2444s		
2455s	2458s			
1725vs	–	–	–	ν(C=O); COOH
–	1617s	1620vs	1627s	$\nu_{as}(COO^-)$
1618vs	1527w	1529vs	1582w	ν(C=O)phenyl breathing modes
1526ms	1496s	1470vs	1524s	
1497s				
1471w	1451vw	–	1473vs	–CH: deformations of CH_2
1456vw				
1413w				
–	1385w	1395vw	1388vs	$\nu_s(COO^-)$
1331s	1335m	1330ms	1328ms	$\delta_b(-CH_2)$
1298vw	1286vw	1281vw		
1257ms	1250m	1254ms	1266s	ν(C–O),
1208s	1200ms	1210m	1203w	ν(C–N),
1166s	1170w	1175vw	1168vw	ν(C–C)
1116m	1093ms,sh	1090m	1133w	$\delta_r(-CH_2)$
1093ms	1042ms,sh	1049m	1090m	
1043s	1014vw		1051ms	
1014m			1024vw	
978w	980vw	929ms	904vw	–CH-bend; phenyl
930s	928s	889m	846w	
889s	890m			
850m	849w			
806ms	807ms			
–	–	–	927vs	ν_{as}(U=O)
–	–	–	810ms	ν_s(U=O)
–	–	808ms	–	ν(Zr=O)
739ms	735ms	740m	737ms	$\delta_b(COO^-)$
650m	655m	653m	660m	ν(M–O) + ring deformation
550w	545w	566w	550vw	
514m	509m	546m	520w	
480w	482vw	454vw	441m	

w = Weak, sh = shoulder, v = very, br = broad, and δ = bending.
[a] s = Strong.
[b] ν = Stretching.

that the hydrogen ions in the lomefloxacin molecules are substituted by the metal ions and the lomefloxacinate is the coordination ligand [14,25,32,33]. The stretching asymmetric (ν_{as}) of carboxylate group between 1617, 1620 and 1627 cm^{-1} and of the symmetric vibrations (ν_s) from 1385 to 1395 cm^{-1} confirm these hypotheses. The band observed at 1618 cm^{-1} in the spectrum of the free lomefloxacin has been assigned before to the stretching vibration of the carbonyl group ν(C=O) [3,25,34–37]. The shift of the carbonyl group to a lower value, Table 2, from 1618 cm^{-1} to 1527 cm^{-1} for Y(III), 1529 cm^{-1} for Zr(IV) and 1582 cm^{-1} for U(VI) indicates coordination of lomefloxacin through oxygen atom of the carbonyl group. The coordination of the metal ions via oxygen carboxylate is confirmed by the ν(M–O) bands at 655, 545 and 509 cm^{-1} for Y(III), 653, 566, 546 and 454 cm^{-1} for Zr(IV) and at 660, 520 and 441 cm^{-1} for U(VI). According to the above discussion the lomefloxacinate is coordinated with the metal ions as bidentate through oxygen atom of carbonyl and one oxygen atoms of carboxylic group.

The stretching vibration $\nu(NH_2^+)$ observed in the spectra of free lomefloxacin and its complexes at almost the same region,

2663–2444 cm^{-1}. The infrared spectra of the prepared complexes display changes in the aromatic ring vibrations in comparison to the corresponding absorption bands for free ligand (Table 2).

For $[UO_2(LFX)_3](NO_3)_2{\cdot}4H_2O$ complex, the most probable structure is shown in Formula 2, where the six oxygen atoms of their LFX ligands occupy equatorial positions around the central metal atom U(VI), forming a plane containing the six-membered rings and the two oxygen atoms of the uranyl group occupy axial positions. The complex possesses one plane of symmetry and no axes of symmetry therefore may have C_s symmetry and are expected to display 459 vibrational fundamentals which are all monodegenerate. These are distributed between motions of the type A′ and A″; all are infrared active. The four vibrations of the UO_2 unit in the complex are of the type 3A′ and A″, these are ν_s(U═O), A′; ν_{as}(U═O), A′; $\delta(UO_2)$, A′ and $\delta(UO_2)$, A″. The data given in Table 2 show that the ν_{as}(U═O) absorption band of this complex occurs as a very strong singlet at 927 cm^{-1} and the ν_s(U═O) absorption band occur at 810 cm^{-1} as a medium strong. These assignments for the stretching vibrations of the uranyl group, UO_2, agree quite well with those known for many dioxouranium(VI) complexes [28,29,38,39]. The ν_s(U═O) value was used to calculate both the bond length and force constant, F(U═O), for the UO_2 bond in our complex according to the known method [39,40]. The calculated bond length and force constant values are 1.732 Å and 641.01 N m^{-1}.

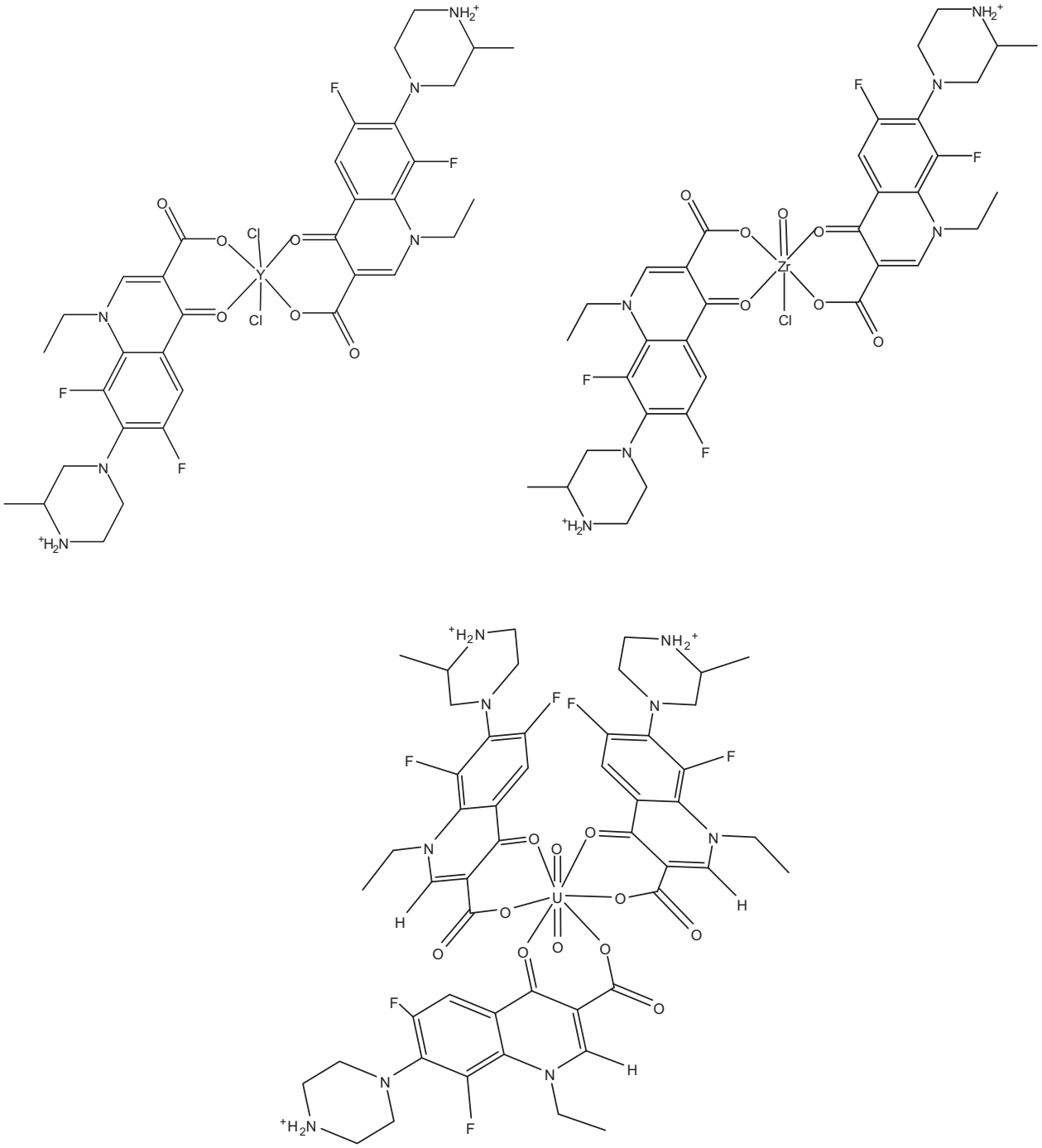

Formula 2. The coordination mode of Y(III), Zr(IV) and U(VI) with lomefloxacin.

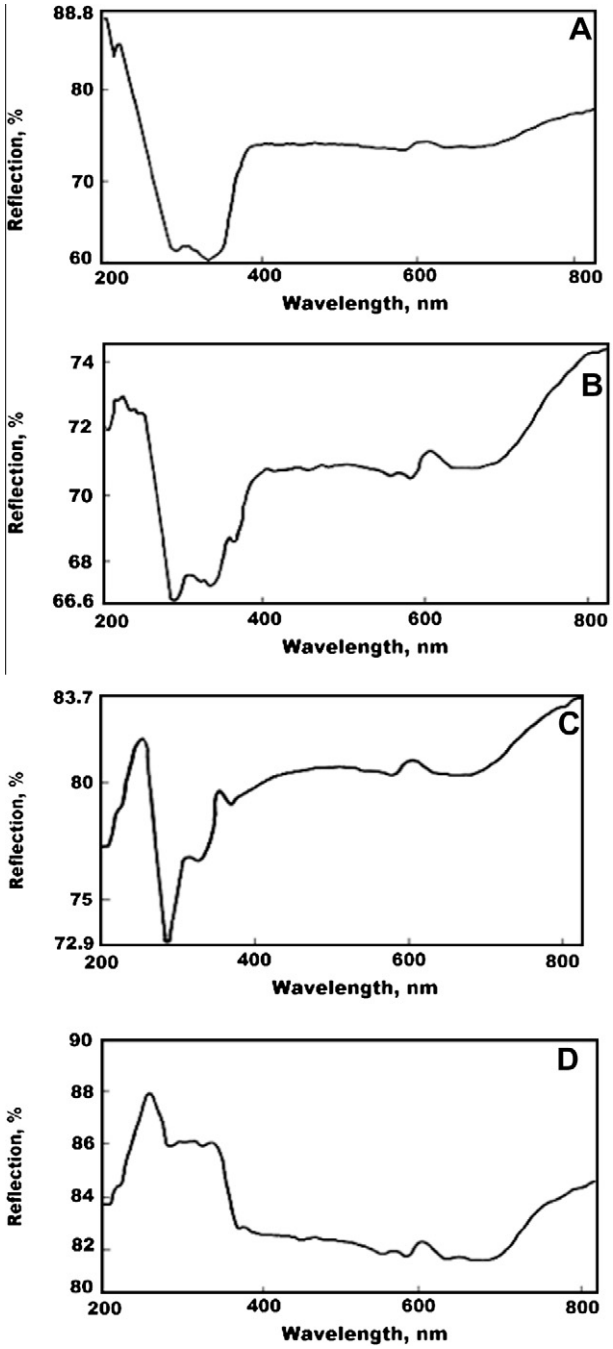

Fig. 2. Electronic reflection spectra of: (A) lomefloxacin (LFX) as a ligand; (B) $[Y(LFX)_2Cl_2]Cl{\cdot}12H_2O$, (C) $[ZrO(LFX)_2Cl]Cl{\cdot}15H_2O$, and (D) $[UO_2(LFX)_3](NO_3)_2{\cdot}4H_2O$ complexes.

Table 3
UV–Vis. spectra of lomefloxacin and its metal complexes (200–800 nm).

Assignments (nm)	LFX	LFX complex with		
		Y(III)	Zr(IV)	U(VI)
π–π^* transitions	214 298	225, 238 248 –	252 –	259 –
n–π^* transitions	304	303, 321 355	311, 355	307, 342 379
Ligand–metal charge-transfer	–	567	566	567

3.2. UV–Vis. spectra

The formation of the metal complexes was also confirmed by UV–Vis. spectra. Fig. 2 shows the electronic solid reflection spectra of free lomefloxacin and its metal complexes and Table 3 reports the reflection spectra from 800 to 200 nm. The reflection spectrum of free lomefloxacin shows bands at 214, 298 and 304 nm which is assigned to π–π^* and n–π^* transitions. For the three complexes the absent of the reflection band at 298 nm and the shift of the other reflectance bands λ_{max} to higher and to lower values attributed to

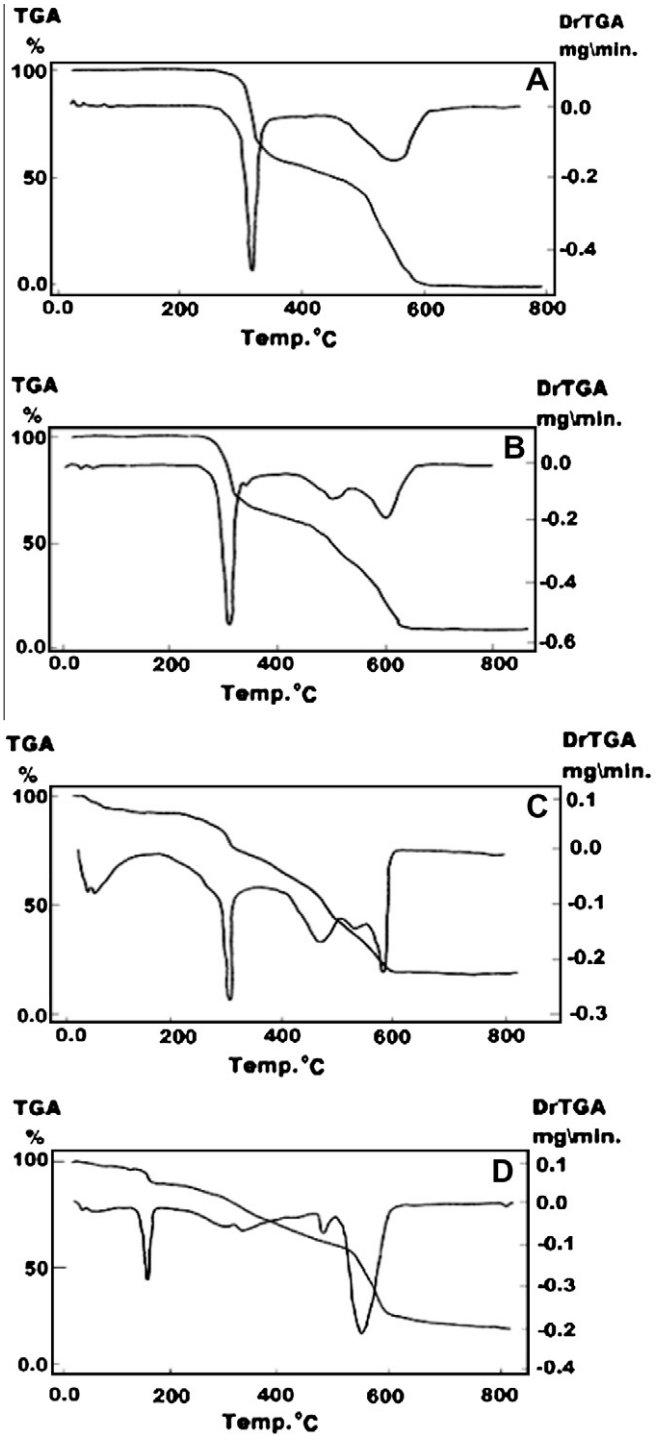

Fig. 3. TGA and DTG diagrams of: (A) lomefloxacin (LFX) as a ligand; (B) $[Y(LFX)_2Cl_2]Cl{\cdot}12H_2O$, (C) $[ZrO(LFX)_2Cl]Cl{\cdot}15H_2O$, and (D) $[UO_2(LFX)_3](NO_3)_2{\cdot}4H_2O$ complexes.

Table 4
The maximum temperature T_{max} (°C) and weight loss values of the decomposition stages for Y(III), Zr(IV), and U(VI) lomefloxacins.

Compounds (MF.)	Decomposition	T_{max} (°C)	Weight loss (%)	
			Calc.	Found
LFX ($C_{17}H_{20}N_3O_3F_2Cl$)	First step	319, 553	100	99.99
	Total loss, residue		100, 0.0	100, 0.0
$[Y(LFX)_2Cl_2]Cl{\cdot}12H_2O$ ($C_{34}H_{62}N_6O_{18}F_4Cl_3Y$)	First step	310, 509, 604	89.86	89.98
	Total loss, residue		89.86, 10.14	89.98, 10.02
$[ZrO(LFX)_2Cl]Cl{\cdot}15H_2O$ ($C_{34}H_{68}N_6O_{22}F_4Cl_2Zr$)	First step	46	7.83	7.82
	Second step	302, 583	71.03	71.19
	Total loss, residue		78.86, 21.14	79.01, 20.99
$[UO_2(LFX)_3](NO_3)_2{\cdot}4H_2O$ ($C_{51}H_{65}N_{11}O_{21}F_6U$)	First step	158	4.74	4.73
	Second step	335, 482, 551	69.59	69.57
	Total loss, residue		74.33, 25.67	74.30, 25.70

complexation behavior of lomefloxacin towards metal ions. The complexes of Y(III), Zr(IV) and U(VI) show new band around 566 nm, which may be assigned to the ligand to metal charge-transfer [3,27–29,34].

3.3. Thermogravimetric analyses

Thermogravimetric (TGA) and differential thermogravimetric (DTG) were carried out for the free lomefloxacin and isolated solid complexes $[Y(LFX)_2Cl_2]Cl{\cdot}12H_2O$, $[ZrO(LFX)_2Cl]Cl{\cdot}15H_2O$ and $[UO_2(LFX)_3](NO_3)_2{\cdot}4H_2O$ under N_2 flow. Fig. 3 represents the TGA and DTG curves and Table 4 gives the maximum temperature values for decomposition along with the corresponding weight loss values for each step of the decomposition reaction. These data support the proposed complexes structures.

Lomefloxacin is thermally stable in the temperature range 25–250 °C. Decomposition of the lomefloxacin started at 250 °C and finished at 600 °C with one stage at two maxima 319 and 553 °C and is accompanied by a weight loss of 99.95%. The hydrated lomefloxacinate of Y(III) is stable up to 245 °C and then decomposed in one step at three maxima 310, 509 and 604 °C to yttrium oxide with intermediate formation of very unstable products which were not identified.

The thermal decomposition of $[ZrO(LFX)_2Cl]Cl{\cdot}15H_2O$ complex proceeds with two main degradation steps. The first stage of decomposition occurs at a temperature maximum of 46 °C. The found weight loss associated with step is 7.82% and may be attributed to the loss of the five water molecules which is in good agreement with the calculated values of 7.83%. The second stage of decomposition occurs at two maxima 302 and 583 °C and the weight loss found at this stage equals to 71.19% corresponds to loss $6C_2H_4 + 4C_2H_2 + 2NH_4Cl + 4HF + 4NO + 4CO + 7H_2O$.

For U(VI) complex the thermal decomposition exhibits two main degradation steps. The first step of decomposition occurs from 30 to 250 °C is accompanied by a weight loss of 4.73% in agreement with the theoretical values 4.74% for the loss of the four uncoordinated water molecules. The second step of decompostion occurs at two maxima 302 and 583 °C with a weight loss of 69.59% this associated with the loss of the three lomefloxacin ligand and nitrate counter ion forming uranium oxide as a final product.

To supporting our conclusion of the absence of all ligand and counter ions and forming metal oxides, we made infrared spectra for the residue of ignition, which clearly shows the bands associated to the metal oxides and disappeared the ban22ds characteristic for the lomefloxacin and counter ions.

According to these conculsions, the decomposition mechansims proposed for LFX and thier complexes are summarized as follows:

The proposed structure formula on the basis of the results discussed in this paper located as shown in Formula 2.

3.4. The kinetic studies

There has been increasing interest in determining rate-dependent parameters of solid-state non-isothermal decomposition reactions by analysis of TGA curves. Several equations have been proposed to analyze a TGA curves and obtain values for kinetic parameters [41–47].

In the present investigation the general thermal behavior of the lomefloxacin ligand and the three complexes in terms of stability ranges, peak temperatures and values of kinetic parameters, are shown in Table 5 (Supplementary data). The kinetic parameters have been evaluated using the following methods and the results obtained by these methods are compared with one another. The following two methods are briefly discussed.

3.4.1. Coats–Redfern equation

The *Coats–Redfern* Eq. (1), which is a typical integral method, can be represented as:

$$\int_0^{\alpha} \frac{d\alpha}{(1-\alpha)^n} = \frac{A}{\varphi}\int_{T1}^{T2} \exp\left(\frac{-E^*}{RT}\right)dT \quad (1)$$

For convenience of integration, the lower limit T_1 is usually taken as zero. This equation on integration gives:

(1) $C_{17}H_{20}N_3O_3F_2Cl \overset{319,553\ ^\circ C}{\rightarrow} 6C_2H_2 + 3CO + C_2H_4 + 2HF + 0.5H_2 + 1.5N_2 + HCl$

(2) $[Y(C_{17}H_{19}N_3O_3F_2)_2Cl_2]Cl \cdot 12H_2O \overset{310,509,604\ ^\circ C}{\rightarrow} YO_{1.5} + 17C_2H_2 + 4HF + 3HCl + 10.5H_2O + 6NO$

(3) $[ZrO(C_{17}H_{19}N_3O_3F_2)_2Cl]Cl \cdot 15H_2O \overset{46\ ^\circ C}{\rightarrow} [ZrO(C_{17}H_{19}N_3O_3F_2)_2Cl]Cl \cdot 10H_2O + 5H_2O$

(4) $[ZrO(C_{17}H_{19}N_3O_3F_2)_2Cl]Cl \cdot 10H_2O \overset{302,583\ ^\circ C}{\rightarrow} ZrO_2 + 10C + 6C_2H_4 + 4C_2H_2 + 2NH_4Cl + 4HF + 4NO + 4CO + 7H_2O$

(5) $[UO_2(C_{17}H_{19}N_3O_3F_2)_3](NO_3)_2 \cdot 4H_2O \overset{158\ ^\circ C}{\rightarrow} [UO_2(C_{17}H_{19}N_3O_3F_2)_3](NO_3)_2 + 4H_2O$

(6) $[UO_2(C_{17}H_{19}N_3O_3F_2)_3](NO_3)_2 \overset{335,482,551\ ^\circ C}{\rightarrow} UO_2 + 10C + 2C_2H_4 + 18C_2H_2 + 6HF + CO + 11NO + 3H_2O + 0.5H_2$

Table 5
Thermal behavior and kinetic parameters determined using the Coats–Redfern (CR) and Horowitz–Metzger (HM) operated for Lomefloxacin and their complexes.

Compounds	Decomposition range (K)	T_s (K)	Method	Parameter					R^a	SD[b]
				E^* (kJ mol^{-1})	A (s^{-1})	ΔS^* (J mol^{-1} K^{-1})	ΔH^* (kJ mol^{-1})	ΔG^* (kJ mol^{-1})		
LFX	523–673	592	CR	137.71	1.242×10^{11}	−38.23	132.79	155.42	0.8885	0.33
			HM	137.97	3.33×10^{11}	−30.03	133.04	150.82	0.8781	0.16
	703–873	695	CR	114.12	6.73×10^{4}	−159.52	108.34	219.21	0.9749	0.17
			HM	102.66	6.27×10^{6}	−121.82	96.88	181.55	0.9886	0.05
$[Y(LFX)_2Cl_2]Cl{\cdot}12H_2O$	523–682	583	CR	97.87	3.02×10^{7}	−107.29	90.30	155.60	0.8149	0.53
			HM	110.77	3.92×10^{8}	−85.91	105.92	156.01	0.8629	0.22
	734–919	782	CR	107.07	2.71×10^{4}	−168.08	100.06	232.01	0.9567	0.17
			HM	82.38	1.27×10^{5}	−155.21	85.88	207.30	0.9833	0.05
$[ZrO(LFX)_2Cl]Cl{\cdot}15H_2O$	299–484	319	CR	18.20	16.19	−222.32	15.55	86.47	0.9464	0.16
			HM	17.87	83.96	−159.58	15.22	66.12	0.9526	0.09
	527–634	575	CR	87.50	7.87×10^{6}	−118.35	82.72	150.77	0.9714	0.16
			HM	98.76	15.87×10^{7}	−93.38	93.98	147.77	0.9775	0.07
$[UO_2(LFX)_3](NO_3)_2{\cdot}4H_2O$	303–523	431	CR	24.03	53.52	−214.88	20.45	113.06	0.9511	0.23
			HM	39.55	74.43	−173.85	35.94	110.87	0.9863	0.06
	540–758	608	CR	40.16	72.25	−215.25	35.10	166.00	0.9774	0.12
			HM	44.24	42.91×10	−200.43	39.18	161.04	0.9721	0.07

[a] Correlation coefficients of the Arrhenius plots.
[b] Standard deviation.

$$\ln\left[\frac{-\ln(1-\alpha)}{T^2}\right] = \frac{-E}{RT} + \ln\left[\frac{AR}{\varphi E^*}\right] \quad (2)$$

A plot of left-hand side (LHS) against $1/T$ was drawn using origin 6.0 program and the fit line is produced. E^* is the energy of activation in kJ mol^{-1} and calculated from the slope and A in (s^{-1}) from the intercept. The entropy of activation ΔS^* in (J K^{-1} mol^{-1}) was calculated by using Eq. (3):

$$\Delta S^* = R\ln\left(\frac{Ah}{K_B T_s}\right) \quad (3)$$

where K_B is the Boltzmann constant, h is the Plank's constant and T_s is the DTG peak temperature [48].

3.4.2. Horowitz–Metzger equation

The *Horowitz–Metzger* equation is an illustrative of the approximation methods. These authors derived the relation:

$$\log\left[\frac{\{1-(1-\alpha)^{1-n}\}}{(1-n)}\right] = \frac{E^*\theta}{2.303RT_s^2} \quad \text{for } n \neq 1 \quad (4)$$

When $n = 1$, the LHS of Eq. (4) would be $\log[-\log(1-\alpha)]$. For a first-order kinetic process the *Horowitz–Metzger* equation may be written in the form:

$$\log\left[\log\left(\frac{W_\alpha}{W_\gamma}\right)\right] = \frac{E^*\theta}{2.303RT_s^2} - \log 2.303 \quad (5)$$

where $\theta = T - T_s$, $w_\gamma = w_\alpha - w$, w_α = mass loss at the completion of the reaction; w = mass loss up to time t. The plot of $\log[\log(w_\alpha/w_\gamma)]$ versus θ was drawn and found to be linear from the slope of which E^* was calculated. The pre-exponential factor, A, was calculated from the equation:

$$\frac{E^*\theta}{RT_s^2} = \frac{A}{\left[\varphi\exp\left(-\frac{E^*}{RT_s}\right)\right]} \quad (6)$$

The entropy of activation, ΔS^*, was calculated from Eq. (3). The enthalpy of activation, ΔH^*, and Gibbs free energy, ΔG^*, were calculated from;

$$\Delta H^* = E^* - RT \quad (7)$$

And

$$\Delta G^* = \Delta H^* - T\Delta S^* \quad (8)$$

It is clear that the thermal decomposition process of the three complexes indicate that the complexes are thermally stable. The positive ΔH^* values postulate an endothermic nature of the formed complexes. The greater negative values of ΔS^* reveal that the three complexes are more ordered with thermodynamic stability. The greater positive values of E^* indicate that the processes involving in translational, rotational, vibrational states and a changes in mechanical potential energy for complexes.

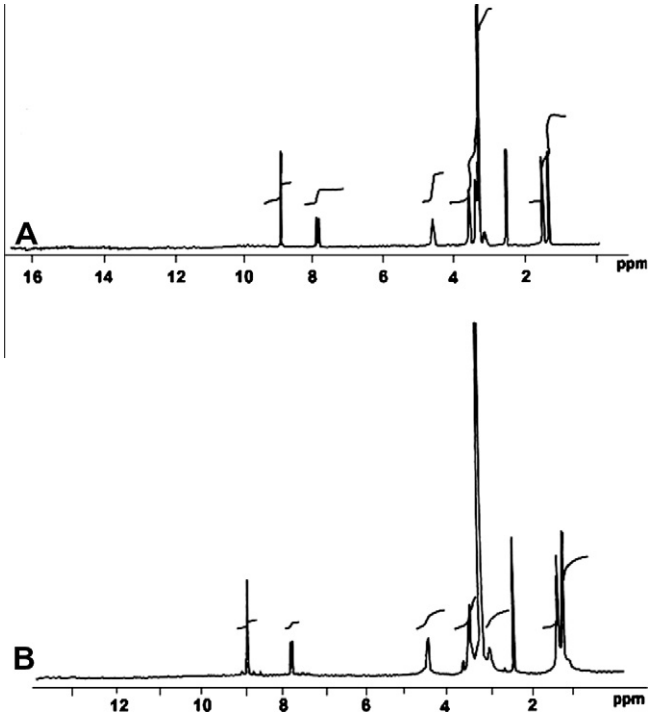

Fig. 4. ^{1}H NMR spectra of: (A) $[Y(LFX)_2Cl_2]Cl{\cdot}12H_2O$ and (B) $[ZrO(LFX)_2Cl]Cl{\cdot}15H_2O$ complexes in DMSO, δ_{TMS}..

Table 6
^{1}H NMR values (ppm) and tentative assignments for: (A) lomefloxacin (LFX) as a ligand; (B) $[Y(LFX)_2Cl_2]Cl{\cdot}12H_2O$, and (C) $[ZrO(LFX)_2Cl]Cl{\cdot}15H_2O$.

A	B	C	Assignments
1.31	1.28, 1.302 1.42, 1.47	1.17, 1.29, 1.37 1.47, 1.52	δH, $-CH_3$
3.51–3.61	3.07, 3.14 3.17, 3.37	3.09, 3.13, 3.32, 3.36	δH, –NH; piperazine
3.98	3.57, 3.59	3.56, 3.74	δH, $-N-CH_2$
–	4.58, 4.59 4.59, 4.61	4.59	δH, H_2O
7.00	7.88	7.87	δH, $-^+NH_2$
7.57, 8.95	7.92, 8.94	7.91, 8.93	δH, $-CH_2$ aromatic
11.00	–	–	δH, –COOH

3.5. The ^{1}H NMR studies

To create harmony between the parts of the study, we embodied the ^{1}H NMR spectra of the lomefloxacin and its complexes with Y(III) and Zr(IV) in Fig. 4. While their peaks assignments are given in Table 6. The ^{1}H NMR spectra of the compounds isolated from systems containing quinolones and metal [26–30,49]; a minor shifts were found. Small shifts could be due to the change in the counter anion or to a different association of the quinolone molecules.

The ^{1}H NMR data for the prepared solid complexes are in agreement with coordination through the carboxylic group (disappeared of the H(COOH) signal in our complexes) and small shifts for all other peaks are shown, thus showing that the magnetic environment of the aromatic rings has changed significantly with coordination. Also, according to the ^{1}H NMR data for $[Y(LFX)_2Cl_2]Cl{\cdot}12H_2O$; δH, H_2O: 4.57, 4.58, 4.59, 4.61 ppm and for $[ZrO(LFX)_2Cl]Cl{\cdot}15H_2O$; δH, H_2O: 4.58 ppm which not found in the free lomefloxacin, indicate the presence of water molecules.

3.6. Antibacterial and antifungal activities

The efficiencies of the lomefloxacin ligand and their metal complexes have been investigated against two Gram-negative, *E. coli* and *P. aeruginosa* and one Gram-positive, *S. aureus*, and antifungal screening was studied against two species such as *P. rotatum* and *T. sp.* microorganisms. The results presented in Table 7 and Fig. 5.

The results of the antibacterial study of the lomefloxacin and the three complexes (Table 7) have inhibitory action against all the three types of bacteria and no antifungal activity for ligand and their metal complexes. All complexes show a good activity against Gram-negative and Gram-positive microorganisms than lomefloxacin and on the other hand, Y(III) complex exhibit excellent activity against Gram-negative, *P. aeruginosa*. The nature of the metal ion coordinated to a drug may have a significant role to this diversity. In general for metal complexes showing antimicrobial activity, the following five principal factors [50–54] should

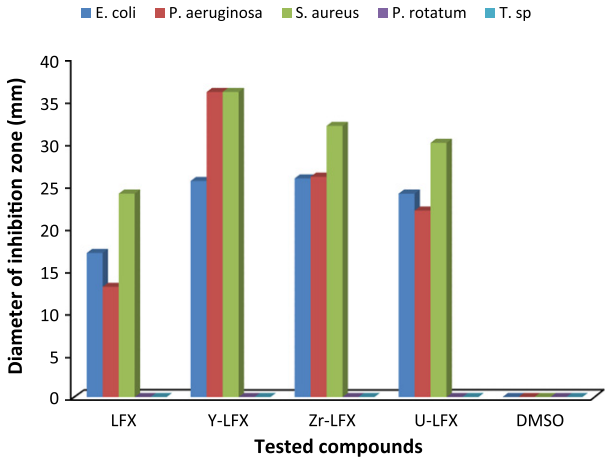

Fig. 5. Statistical representation for biological activity of lomefloxacin and its complexes.

be considered: (i) the chelate effect; (ii) the nature of the ligands; (iii) the total charge of the complex; (iv) the nature of the ion neutralizing the ionic complex; and (v) the nuclearity of the metal center in the complex. All of the five above mentioned factors are present to our compounds except the second factor.

4. Conclusion

Three new Y(III), Zr(IV) and U(VI) complexes with lomefloxacin (LFX) in ethanol, methanol and acetone as a solvent have been synthesized. Elemental analysis, infrared, ultraviolet–visible, nuclear magnetic resonance, conductance measurements and thermogravimetric (TGA) and differential thermal analyses (DTG) have been used to characterize the isolated solid complexes. The kinetic parameters of thermogravimetric (TGA) and its differential (DTG), such as entropy of activation, energy of activation, enthalpy of activation and Gibbs free energy evaluated by using the Coats–Redfern and Horowitz–Metzeger equations. The bond stretching force constant and length of the U=O bond for the $[UO_2(LFX)_3](NO_3)_2{\cdot}4H_2O$ complex were calculated. Antimicrobial studies were carried out against several bacterial and fungal species. The results showed significant increase in antibacterial activity of metal complexes as compared with free ligand and no antifungal activity observed for ligand and their complexes.

Appendix A. Supplementary material

Supplementary data associated with this article can be found, in the online version, at doi:10.1016/j.molstruc.2010.07.041.

Table 7
The inhibitation diameter zone values (mm) for LFX and its compounds.

Compounds	Microbial species				
	Bacteria			Fungi	
	E. coli	*P. aeruginosa*	*S. aureus*	*T. sp*	*P. rotatum*
LFX	17 ± 0.1155	13 ± 0.2887	24 ± 0.2309	0	0
$[Y(LFX)_2Cl_2]Cl{\cdot}12H_2O$	25.5^{+2} ± 0.2887	36^{+3} ± 0.3464	36^{+3} ± 0.1472	0	0
$[ZrO(LFX)_2Cl]Cl{\cdot}15H_2O$	25.8^{+2} ± 0.1155	26^{+2} ± 0.4041	32^{+2} ± 0.7044	0	0
$[UO_2(LFX)_3](NO_3)_2{\cdot}4H_2O$	24^{+2} ± 0.4619	22^{+2} ± 0.201	30^{+2} ± 0.3464	0	0
Control (DMSO)	0	0	0	0	0

Statistical significance: $^{(NS)}$ not significant, $P < 0.05$; $^{(+1)}$ significant, $P > 0.05$; $^{(+2)}$ highly significant, $P > 0.01$; $^{(+3)}$ very highly significant, $P > 0.001$; student's *t*-test.

References

[1] D.H. Brown, W.E. Smith, J.W. Teape, J. Med. Chem. 23 (1980) 729.
[2] R.J. Anacona, T. Caredmy, Transition Met. Chem. 26 (2001) 228–231.
[3] N. Sultana, A. Naz, M.S. Arayne, M.A. Mesaik, J. Mol. Struct. 969 (2010) 17–24.
[4] L.A. Mitscher, Chem. Rev. 105 (2005) 559.
[5] T.D. Gootz, J.F. Barrett, J.A. Sutcliffe, Antimicrob. Agents Chemother. 34 (1990) 8.
[6] K. Hoshino, A. Kitamura, I. Morrissey, K. Sato, J. Kato, H. Ikeda, Antimicrob. Agents Chemother. 38 (1994) 2623.
[7] J. Chamani, N. Tafrishi, M. Momen-Heravi, J. Lumin. 130 (2010) 1160–1168.
[8] D.L. Ross, C.M. Riley, Int. J. Pharmaceut. 87 (1992) 203–213.
[9] L. Jian-Quan, F. Jin, S. Ting-Quan, Z. Xing-Wang, Int. J. Biol. Macromol. 40 (2007) 299–304.
[10] S.C. Wallis, L.R. Gahan, B.G. Charles, T.W. Hambley, Aust. J. Chem. 47 (1994) 799.
[11] I. Turel, K. Gruber, I. Leban, N. Bukovec, J. Inorg. Biochem. 61 (1996) 197.
[12] M. Czugler, G. Argay, J. Frank, Z. Meśzaŕos, L. Kutschabsky, G. Reck, Acta Crystallogr. B 32 (1976) 3124.
[13] M. Cygler, C.P. Huber, Acta Crystallogr. C 41 (1985) 1052.
[14] C.M. Riley, D.L. Ross, D.V. Velde, F. Takusagawa, J. Pharmaceut. Biomed. 11 (1993) 49.
[15] L. Golič, B. Šuštar, M. Barbo, in: Joint Slovenian–Croatian Crystallographic Meeting, Otočec Book of Abstracts, 1992, p. 25.
[16] A.J. Florence, A.R. Kennedy, N. Shankland, E. Wright, A. Al-Rubayi, Acta Crystallogr. C 56 (2000) 1372.
[17] I. Turel, P. Bukovec, M. Quiroś, Int. J. Pharmaceut. 152 (1997) 59.
[18] A. Sivalakshmidevi, K. Vyas, G. Om Reddy, Acta Crystallogr. C 56 (2000) e115.
[19] J. Chem. Soc. Dalton Trans. 22 (2000) 4013.
[20] I. Turel, L. Leban, G. Klintschar, N. Bukovec, S. Zalar, J. Inorg. Biochem. 66 (1997) 77.
[21] M. Ruiz, R. Ortiz, L. Perello, J.S. Carrio, J. Inorg. Biochem. 65 (1997) 87.
[22] M. Ruiz, L. Perello, R. Ortiz, A. Castineiras, C.M. Mossmer, E. Canton, J. Inorg. Biochem. 59 (1995) 801.
[23] B. Macias, M.V. Villa, I. Rubio, A. Castineiras, J. Borras, J. Inorg. Biochem. 84 (2001) 163.
[24] I. Turel, I. Leban, N. Bukovec, J. Inorg. Biochem. 66 (1997) 241.
[25] K. Nakamoto, Infrared and Raman Spectra of Inorganic and Coordination Compounds, fourth ed., Wiley, New York, 1986. pp. 230.
[26] S.A. Sadeek, J. Mol. Struct. 753 (2005) 1.
[27] S.A. Sadeek, M.S. Refat, H.A. Hashem, J. Coord. Chem. 59 (2006) 7.
[28] S.A. Sadeek, W.H. EL-Shwiniy, J. Mol. Struct. 977 (2010) 243–253.
[29] S.A. Sadeek, W.H. EL-Shwiniy, J. Coord. Chem. (2010).
[30] S.A. Sadeek, W.H. EL-Shwiniy, W.A. Zordok, A.M. EL-Didamony, J. Argent. Chem. Soc. 97 (2009).
[31] D.J. Beecher, A.C. Wong, Appl. Environ. Microbiol. 60 (1994) 1646–1651.
[32] W. Brzyska, M. Hakim, Pol. J. Chem. 66 (1992) 413.
[33] G. Kumar, M. Srivastava, Rev. Chim. Miner. 16 (1979) 14.
[34] E.K. Efthimiadou, A. Karaliota, G. Pasomas, J. Inorg. Biochem. 104 (2010) 455–466.
[35] E.K. Efthimiadou, A. Karaliota, G. Pasomas, Polyhedron 27 (2008) 349.
[36] E.K. Efthimiadou, Y. Sanakis, C.P. Raptopoulou, A. Karaliota, N. Katsaros, G. Pasomas, Bioorg. Med. Chem. Lett. 16 (2006) 3864.
[37] E.K. Efthimiadou, M.E. Katsarou, A. Karaliota, G. Pasomas, J. Inorg. Biochem. 102 (2008) 910.
[38] S.A. Sadeek, S.M. Teleb, M.S. Refat, M.A.F. Elmosallamy, J. Coord. Chem. 58 (2005) 1077.
[39] S.P. Mcglynnm, J.K. Smith, W.C. Neely, J. Chem. Phys. 35 (1961) 105.
[40] L.H. Jones, Spectrochim. Acta 15 (1959) 409.
[41] E.S. Freeman, B. Carroll, J. Phys. Chem. 62 (1958) 394.
[42] J. Sestak, V. Satava, W.W. Wendlandt, Thermochim. Acta 7 (1973) 333.
[43] A.W. Coats, J.P. Redfern, Nature 201 (1964) 68.
[44] T. Ozawa, Bull. Chem. Soc. Jpn. 38 (1965) 1881.
[45] W.W. Wendlandt, Thermal Methods of Analysis, Wiley, New York, 1974.
[46] H.W. Horowitz, G. Metzger, Anal. Chem. 35 (1963) 1464.
[47] J.H. Flynn, L.A. Wall, Polym. Lett. 4 (1966) 323.
[48] P. Kofstad, Nature 179 (1957) 1362.
[49] J.H. Flynn, L.A. Wall, J. Res. Natl. Bureau Stand. 70A (1996) 487.
[50] B. Macıàs Sańchez, M. Martinez Cabarga, A. Sańchez Navarro, A. Dominguez-Gil Hurlé, Int. J. Pharmaceut. 106 (1994) 229.
[51] G. Pasomas, C. Dendrinou-Samara, P. Philippakopoulos, V. Tangoulis, C.P. Raptopoulou, E. Samaras, D.P. Kessissoglou, Inorg. Chim. Acta 272 (1998) 24–32.
[52] C. Dendrinou-Samara, G. Pasomas, C.P. Raptopoulou, D.P. Kessissoglou, J. Inorg. Biochem. 83 (2001) 7–16.
[53] A.D. Russell, in: S.S. Block (Ed.), Disinfection, Sterilization and Preservation, fourth ed., Lea and Febinger, Philadelphia, 1991. pp. 27–59.
[54] H.W. Rossmore, in: S.S. Block (Ed.), Disinfection, Sterilization and Preservation, fourth ed., Lea and Febinger, Philadelphia, 1991. pp. 290–321.